Pharm Res (2012) 29:2128–2138
DOI 10.1007/s11095-012-0742-4

RESEARCH PAPER

The Development of Thermal Nanoprobe Methods as a Means of Characterizing and Mapping Plasticizer Incorporation into Ethylcellulose Films

Jin Meng • Marina Levina • Ali R. Rajabi-Siahboomi • Andrew N. Round • Mike Reading • Duncan Q. M. Craig

Received: 7 September 2011 / Accepted: 19 March 2012 / Published online: 14 April 2012

ABSTRACT

Purpose The phase composition and distribution of ethylcellulose (EC) films containing varying amounts of the plasticizer fractionated coconut oil (FCO) were studied using a novel combination of thermal and mapping approaches.

Methods The thermal and thermomechanical properties of films containing up to 30% FCO were characterized using modulated temperature differential scanning calorimetry (MTDSC) and dynamic mechanical analysis (DMA). Film surfaces were mapped using atomic force microscopy (AFM; topographic and pulsed force modes) and the composition of specific regions identified using nanothermal probes.

Results Clear evidence of distinct conjugate phases was obtained for the 20–30% FCO/EC film systems. We suggest a model whereby the composition of the distinct phases may be estimated via consideration of the glass transition temperatures observed using DSC and DMA. By combining pulsed force AFM and nano-thermal analysis we demonstrate that it is possible to map the two separated phases. In particular, the use of thermal probes allowed identification of the distinct regions via localized thermomechanical analysis, whereby nanoscale probe penetration is measured as a function of temperature.

Conclusion The study has indicated that by using thermal and imaging techniques in conjunction it is possible to both identify and map distinct regions in binary films.

J. Meng • A. N. Round • M. Reading • D. Q. M. Craig (✉)
School of Pharmacy, University of East Anglia
Norwich, UK NR4 7TJ
e-mail: d.craig@uea.ac.uk

M. Levina • A. R. Rajabi-Siahboomi
Colorcon Limited, Flagship House
Victory Way, Crossways, Dartford
Kent DA2 6QD, UK

KEY WORDS atomic force microscopy · ethylcellulose · film coating · phase separation · plasticizers · thermal analysis

INTRODUCTION

The incorporation of low molecular weight molecules into polymers is of crucial importance, not just for the polymer industry but also for fields such as pharmaceutical development whereby there is an increasing interest in the use of drug dispersions in water-miscible polymers as a means of enhancing bioavailability (1). In general terms, molecules such as plasticizers, dyes, opacifiers, preservatives and flavours may all be incorporated (2); in each case the performance of the composite material will be strongly dependent on the nature of the incorporation and the accompanying physical stability of the binary system.

The physical structure of such mixed systems may be remarkably complex. In the simplest case the incorporated molecule may be molecularly dispersed, in which case characterization is relatively straightforward. Methods such as differential scanning calorimetry (DSC) or dynamic mechanical analysis (DMA) may be utilized to measure the glass transition temperature (T_g) of the composite in relation to those of the constituent materials. Hence one may ascertain not only the miscibility but also the level of interaction between the additive and the polymer using relationships such as the Gordon-Taylor equation (3). However, in most practical cases it is necessary to consider the saturation, supersaturation and phase separation of the incorporated molecules. Indeed, compatibility (used in the sense of stable miscibility) prediction has long been an important field, particularly in terms of plasticizer incorporation. Plasticizers alter the mechanical properties of the host polymer, typically including greater flexibility, greater elongation potential,

higher impact resistance but lower tensile strength. They also lower the glass transition of the host polymer, although the interrelationship between these phenomena is still not fully understood (4,5).

There are a number of theories regarding the mechanisms underpinning plasticization (4,5). Originally, it was thought that the plasticizers behaved as molecular lubricants and/or acted to increase mobility within the three dimension gel-like structure of the polymer. However the increased understanding of the nature of the glass transition led to emphasis on how the lowering of T_g could be explained in terms of the free volume theory (6). In brief, it was noted that most polymers undergo T_g at approximately the same viscosity (circa 10^{12} Pa.s). This observation led to the concept of the fractional free volume which decreases as the temperature is lowered to a critical value at which T_g would then occur. It was proposed that addition of the plasticizer not only resulted in the presence of molecules with a lower T_g but that such molecules also act to increase the free volume, both effects resulting in a lowering of the T_g. This explanation does not fully account for the observed changes in mechanical properties, nor does it explain phenomena such as antiplasticization (whereby small quantities of plasticizer may increase the T_g) or the anomalous relationship between molecule free volume of the plasticizer and the lowering of T_g. However, Sears and Darby (5) have suggested that polymers may contain ordered regions (crystallites) which are to a large extent responsible for the mechanical properties of the polymer, with the plasticizers possibly altering the distribution of these structures as well as altering the free volume of the wholly amorphous regions.

In terms of the measurement of plasticization and the selection of the most suitable agent, these issues may be considered in terms of the development of theoretical approaches to predict suitability and practical validation of such models. In terms of the former, the well-known Flory-Huggins approach (7) considers the miscibility of additives with polymers in terms of the thermodynamics of mixing, while a second related approach involves the use of the solubility parameter δ (8), which is a measure of the cohesive energy density of a component. This parameter is frequently used to predict miscibility on the basis that these values are essentially molecular interaction parameters; hence knowledge of the values for the two components in theory leads to prediction of likely miscibility.

A basic difficulty associated with measuring miscibility is that, unlike examination of solid dissolution in liquids, practical assessment of miscibility in solid polymers is a non-trivial undertaking, yet such information is essential in order to verify theoretical approaches. Techniques for detecting solid material in crystalline or amorphous form include thermal approaches, spectroscopic methods and imaging approaches such as scanning electron microscopy (SEM; 9–11). However there is a significant issue in either sensitivity or in verifiability with each of these approaches. More specifically, methods such as DSC may not be able to detect very small quantities of one material in another, while methods such as AFM may detect the presence of incongruous structures but positive identification of those structures, in the light of their possibly being merely topographical features, may be considerably more difficult. A further complication is that, while solid-liquid systems may exhibit supersaturation for a limited time period, such supersaturation may be kinetically quite stable in polymers, rendering reliable measurements of equilibrium miscibility problematic (9,11).

This study concerns the widely used polymer ethylcellulose, a semi-synthetic derivative of cellulose whereby the ethylation process confers water immiscibility. Typically, EC has ethoxyl substitution between 44 and 51%, with the flexibility and glass transition temperature decreasing with substitution (12). The polymer is generally considered to be highly amorphous with a glass transition circa 129–133°C, although Bhedfa *et al* (13) have reported lyotropic liquid crystalline properties and Lai *et al* (12) have suggested the presence of microcrystals within the amorphous matrix which may exhibit a melting endotherm at elevated temperatures. The polymer is widely used in the food, cosmetic and insulation industries. One of the main applications, however, is in the pharmaceutical field whereby EC is used as a barrier membrane coating for controlled release dosage forms. More specifically, the water immiscibility of the polymer slows drug release within the gastrointestinal tract. The presence of "micro-defects" in the film and incorporation of permeability enhancers (commonly referred to as pore forming agents or indeed plasticizers) may tailor the release to the desired characteristics. EC alone is a very brittle material and not suited to coating of irregularly shaped materials, hence inclusion of a plasticizer is essential for practical purposes.

As outlined above, while it is relatively simple to assess the macroscopic and bulk structural properties of plasticized polymers, it is more difficult to identify the point at which phase separation may occur and to characterize the spatial distribution of these binary systems. This is of considerable practical importance, as long term stability is a key performance parameter for almost all polymeric products and is particularly important for pharmaceuticals whereby products are highly regulated for reasons of patient safety. A greater understanding of how phase separation may be assessed and hence anticipated or prevented would therefore be of considerable use within the field. In the current study we present a unique combination of thermal, thermomechanical and imaging approaches to study the incorporation of the plasticizer, fractionated coconut oil (FCO), into EC films. FCO is used commercially in pharmaceutical films and comprises the medium chain saturated fatty acid

fraction of coconut oil, consisting mainly of caprylic (8 carbon) and capric (10 carbon) acids. It therefore represents both a practically relevant material as well as one with phase separation tendencies that lend the associated systems to technique development for detection and quantification of the separation process. Here we use modulated temperature DSC (MTDSC) in first derivative mode to measure the glass transitional behaviour of the polymer systems, dynamic mechanical analysis to measure the thermomechanical properties and a combination of atomic force microscopy (AFM) and nanothermal analysis to map the distribution of the phase separated material. Nanothermal analysis is a relatively new technique whereby the tip of an AFM is replaced by a miniaturised silica-based thermistor. In the simplest mode, the probe may be placed on a region of interest, the temperature of the probe increased and the probe displacement measured as it moves through the sample on softening, thereby allowing measurement of the temperature of the transition (14,15). There are numerous variations on this premise, using both nanoprobes and the preceding microprobes, which allow a wider range of modalities, including three dimensional mapping, photothermal IR and single particle analysis (16,17). Overall, however, the significant advantage of this method is that it allows thermal analysis to be performed on highly specific regions of a sample, thereby opening the possibility of both identification of features in binary systems and verification of their chemical or physical nature. In this investigation, therefore, we intend to both identify immiscibility and/or phase separation between the polymer and plasticizer and also to map how that separation manifests itself on a nanoscale.

MATERIALS AND METHODS

Materials and Preparation of EC Films

Ethylcellulose (ETHOCEL^{TM} 20) was donated by Colorcon (West Point, PA, USA). Fractionated coconut oil (FCO) was obtained from Abitec Corporation (Columbus, OH, USA). 20 mL of 10% (w/v) ethylcellulose solutions were prepared by dissolving 2 g polymer powder in 20 mL ethanol/acetone (60/40 v/v), with the specified level of plasticizer then added. Fractionated coconut oil was incorporated at concentrations of 0%, 5%, 10%, 15%, 20%, 25% and 30% (w/w of EC). The ethylcellulose solutions were heated to 45°C on a hot plate and magnetically stirred until the polymer was fully dissolved. Parafilm was used to limit the evaporation of solvents during the stirring. After stirring, the solution was rested on the hot plate for another 5 minutes to allow the escape of air bubbles. Films were obtained by casting solutions on a glass plate by using a REF 1117 film applicator (Sheen Instruments Ltd., Survey, England). The wet film thickness was controlled at 2500 μm by adjusting the micrometers of the film applicator. The films were dried at 50°C (Gallenkamp Vacuum Oven, Fistreem International Ltd.) for 3 hours. Clear, dry films were obtained which were stored over silica gel prior to analysis.

Residual Solvents and Degradation

Thermogravimetric analysis (TGA; TA Instruments 2950, Delaware, US) was used to determine the solvent residue and degradation of dry films. The samples were heated from room temperature to 350°C at 10°C/min. Both the weight loss and derivate weight loss signals were used to analyze the onset of degradation. The sample weight was approximately 10 mg. Dry nitrogen was used as the purge gas and compressed air as the cooling system.

Modulated Differential Scanning Calorimetry (MTDSC)

MTDSC experiments were conducted from 20°C to 220°C with a modulation amplitude of ±0.5°C and a period of 40 seconds at a heating rate of 2°C/min using DSC Q1000 (TA Instruments, Delaware, USA) with a refrigerated cooling system (RCS) accessory. The sample mass was 2–5 mg and pin-holed crimped pans were used. Indium (T_m=156.6°C), tin (T_m=231.9°C) and n-octadecane (T_m=28.2°C) were used as the standard temperature calibrants. Heat capacity calibration was performed using Al_2O_3 dry powder according to the same program as for the samples. The DSC cell was purged with 50 cm^3/min dry nitrogen and the RCS with 150 cm^3/min nitrogen. All experiments were performed in triplicate. The derivative heat capacity signals were plotted against temperature and the consequent plots were smoothed at 3°C increments using Universal Analysis software (TA Instruments, Delaware, USA).

Dynamic Mechanical Analysis (DMA)

DMA was used in a tension mode (tensile clamp) (DMA 2980, TA Instruments, USA) in order to investigate the storage modulus, loss modulus and tan δ of the samples as a function of temperature. The films were cut into 30× 5.27 mm square pieces and then mounted on the fixed clamps. Two clamp screws were tightened by using the torque wrench to the appropriate torque (3-5 in-lbs). Samples were heated from 30°C to 180°C at a rate of 3°C/min under the parameters of frequency 1 Hz, amplitude 20 μm, static force 0.05 N and auto-strain of 120%. Dry filtered air was used as purge gas and cooling system. Before the experiments were started, a set of calibrations were carried out (position, force, clamp, electronic and temperature). Each experiment was carried out in triplicate.

Pulsed Force, Atomic Force Microscopy (AFM) and Nano-Thermal Analysis

In this set of studies, AFM (fitted with a heated stage) was used to image the surface of samples in topographic and pulsed force mode. Images at a stage temperature of 45°C were obtained in order to explore whether raising the temperature could enhance contrast. However, this was found not to be the case and hence this avenue of exploration was not taken further.

Nano-thermal studies were used to image the sample at room temperature in the first instance and then to perform localised thermomechanical analysis studies on selected point regions. An attempt was made to image the surface as a function of temperature using the nanothermal probes but the tips were easily damaged or contaminated when mapping in this mode. Consequently, mapping was only performed at room temperature using these tips.

Heated Stage AFM

A Thermomicroscopes Explorer scanning probe microscope (Anasys Instruments, Santa Barbara, CA, USA) was applied to image the film surfaces. The heated stage was used to control the temperature at 25°C (and 45°C) by applying a Linkam TP93 controller (Linkam Scientific Instruments, Surrey, UK) with a heating rate of 10°C/min. The AFM images were taken using the pulse force probes at the above temperatures with a set point of 10 nA. The frequency and amplitude for modulation and subtracted baseline were 500 Hz and 50 nm respectively. The scan area was 25×25 μm and the scan speed was 19.9 μm/s with 200 lines of resolution. Five repeats were performed on different regions of the prepared films. For each region, five points were chosen on which to perform the AFM studies. Good reproducibility was found in all cases.

Nano-Thermal Analysis (nanoTA)

A NanoTA Thermal Analyzer combined with Thermomicroscopes Explorer scanning probe microscope (pulsed force mode, Anasys Instruments, Santa Barbara, CA, USA) was utilized. Pulsed force mode mapping was used to identify the different regions and then localized thermomechanical analysis to assess the probe penetration area on selected regions. The system was calibrated with respect to probe penetration using polyethylene (T_m=55°C), polyethyelene terephthalate (T_m=130°C) and polycaprolactone (T_m=238°C). The film samples were mounted onto metal sample studs and placed on the stage. The surfaces of the films (in 5 μm^2 regions) were scanned initially to obtain the topography and adhesion images (by using the nanoprobes in pulsed force mode). The nanoTA thermal probe was then positioned on specific areas as indicated. Localized thermal analysis (LTA) data were obtained at 5°C/s between room temperature and 150°C, whereby probe cantilever deflection was plotted against probe tip temperature on those specific regions. Previous investigations studies have indicated that such studies interrogate regions of circa 250 nm×250 nm (14). The basic settings were the same as those used in the pulsed force mode/heated stage AFM; 5 μm×5 μm regions were scrutinised. Thermal analysis data was obtained at 5°C/s between room temperature and 150°C. Probe cantilever deflection was plotted against probe tip temperature to obtain the glass transition temperatures (T_gs) of specific areas on the film surfaces. Five repeats were performed on different regions of the films.

RESULTS

Residual Solvents and Degradation Studies

In order to verify subsequent experimental studies, it was considered important to ascertain both the residual solvent levels and the tendency for the systems to degrade in terms of whether there is significant weight loss over the temperature ranges under study. TGA (unless coupled with a more specific analytical method) is not able to specifically identify materials that are being lost but nevertheless provides a useful insight into the temperature dependence of the degradation process. This is particularly pertinent for plasticized systems as many are volatile and may therefore be lost during experimental analysis (18).

The weight loss profile for FCO/EC films is shown in Fig. 1. Close examination of the data (not highlighted) indicates that there appears to be a low temperature weight loss of circa 0.67% that it is reasonable to ascribe to residual solvent. The dry films had a main degradation onset temperature at circa 180°C which is some 70°C lower than that of pure EC (250°C), while FCO alone degraded from circa 120°C (data not shown). It is therefore concluded that there is an acceptably small level of residual solvent in the sample and that over the temperature range under study it is unlikely that significant sample degradation will be present.

Modulated Temperature Differential Scanning Calorimetry (MTDSC) Studies

MTDSC involves the application of a modulated (in this case sinusoidal) heating signal to a sample superimposed upon the underlying heating rate, thereby allowing the reversing heat capacity to be obtained from the modulation in isolation from accompanying kinetic events. A further advantage of MTDSC, which we exploit here, is that the use of the sine wave to derive heat capacity (C_p), with the

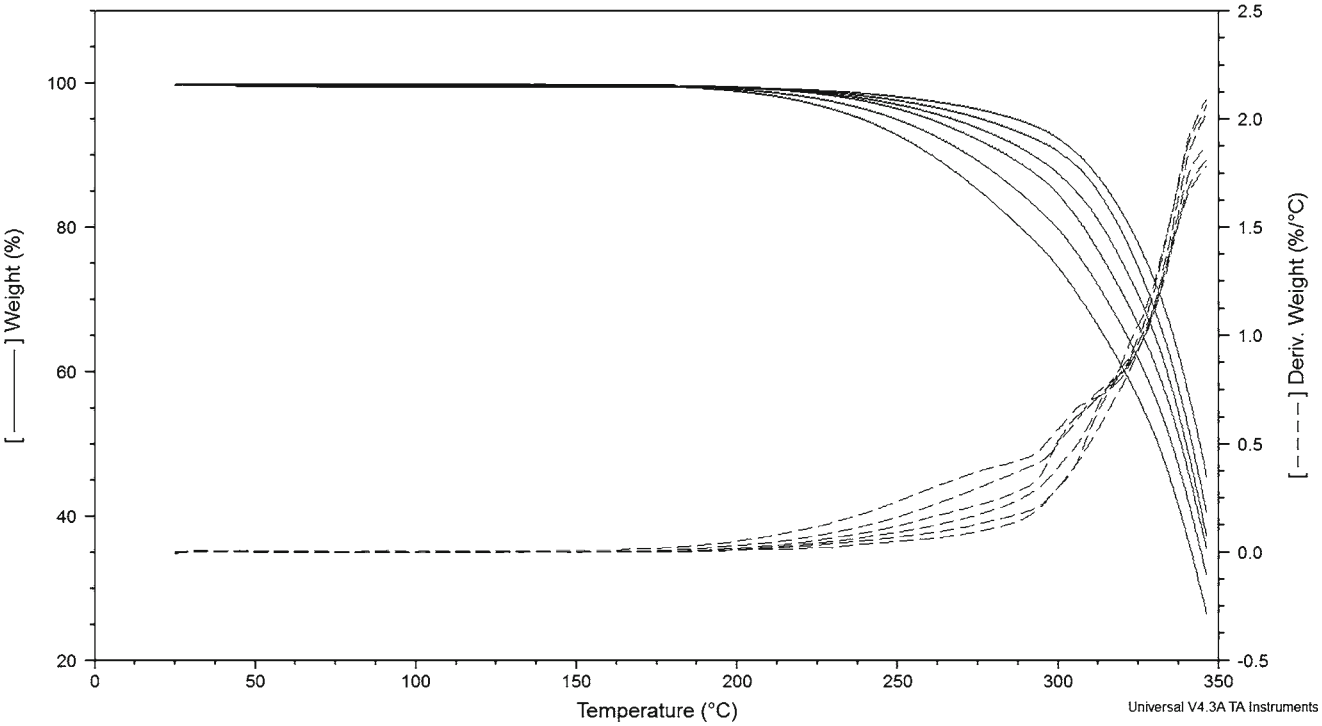

Fig. 1 TGA analysis (weight as % of starting value and derivative of same) for ethylcellulose films containing up to 30% fractionated coconut oil. The weight loss curves (solid lines) from top to bottom: 0, 5, 10, 15, 20, 25, 30% w/w FCO. The derivative weight loss curves (dashed lines) show this order in reverse.

accompanying range of heating rates during a single cycle, allows a much improved signal to noise and hence greater baseline stability for measuring subtle transitions (19).

The heat capacity change (ΔC_p) associated with the T_g of EC is known to be small (12), thus rendering detection and/or assessment of ΔCp difficult, particularly if further components are present which will decrease the absolute response per total weight of a sample. On this basis, the derivative reversing heat capacity signals are used here, whereby the glass transition will appear as a peak against the derivative baseline. The corresponding signals from MTDSC scans of EC films and those with 0%, 5%, 10%, 15%, 20%, 25% and 30% FCO are shown in Fig. 2. The value of T_g for the EC film was 129.2± 0.1°C, which is in reasonable agreement with previous studies (12). An endothermic event was observed around 180°C which was consistent with observations by Lai *et al* (12) who ascribed this to melting of micro crystallites in the EC (this endotherm is expressed as an upward then downward peak in the derivative signal).

On addition of the plasticizer, the T_g decreased as expected (Table I), but at 20% and beyond, the T_g value remained reasonably constant at circa 97°C while a further lower temperature peak was observed at circa 53°C. Hence two transitions are seen which do not correspond to either individual component. Phase separation may therefore not comprise simply the presence of individual components but may instead reflect mixed phases. This will be discussed further in a subsequent section.

Dynamic Mechanical Analysis (DMA) Studies

Figure 3a and b show the corresponding DMA data for the EC films on addition of FCO. It was found that at high temperatures, the storage moduli of the films became so low that reliable measurement was no longer possible. On examination of the effects of addition of FCO, the following were apparent. Firstly, the storage modulus of the films decreased (Fig. 3a), as one would expect on addition of a plasticizer (20–22). Such effects are well known and are typically accompanied by a decrease in tensile modulus and strength and increased elongation at break (20). Secondly, by examining the tan δ value it is possible to derive the glass transition temperature (typically taken as the peak in tan δ). Furthermore, by examining the width of the tan δ peak it is possible to derive information regarding the heterogeneity of the relaxation time (23). In the present case the difficulties associated with post-T_g measurement resulted in the complete peak not being measurable, hence the relaxation behaviour was not easily assessed, although it was possible to derive the T_g values for these systems. These are shown in Table I. It was noted that a pre-peak discontinuity in the tan δ value was seen, which we suggest

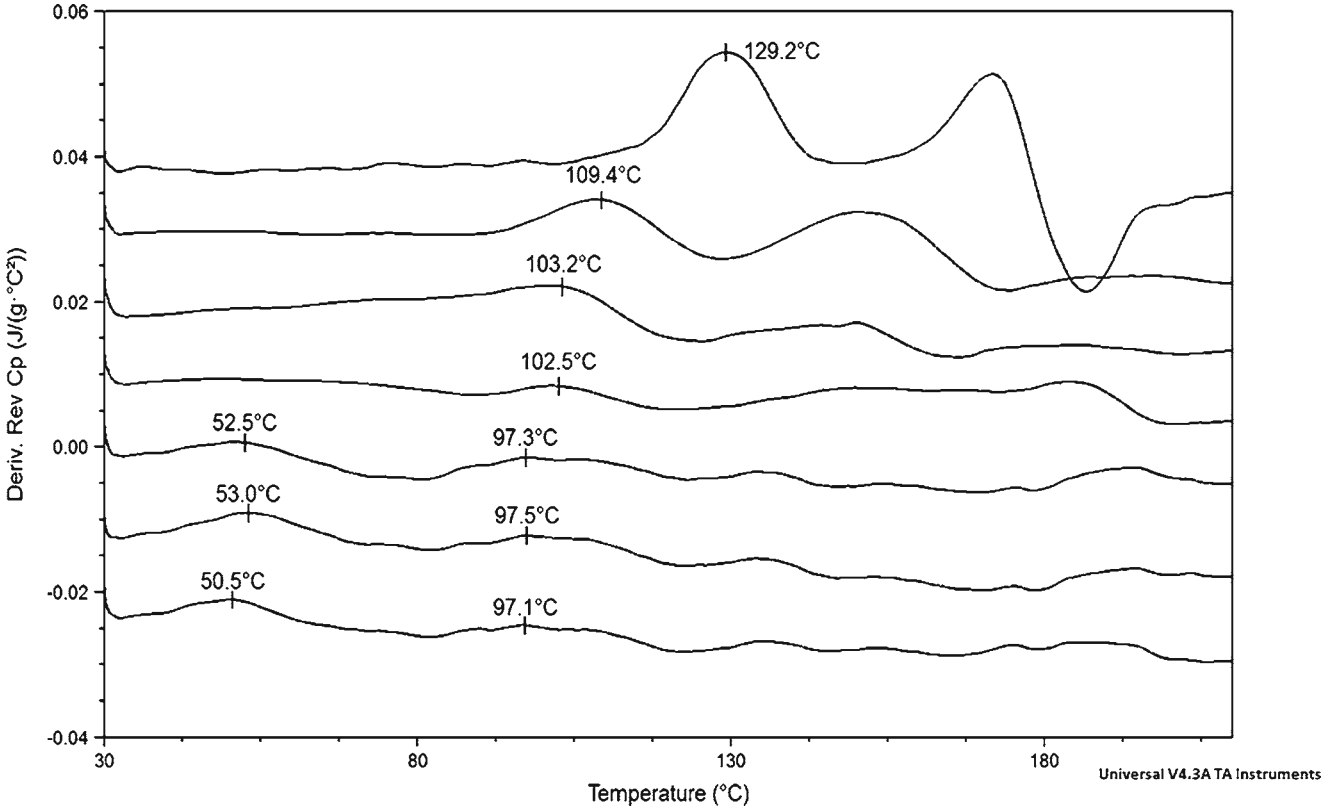

Fig. 2 Derivative MTDSC (reversing heat capacity) response of ethylcellulose with added FCO at concentrations 0, 5, 10, 15, 20, 25, 30% w/w from top to bottom.

corresponds to a second glass transition, for the 20% FCO film. However, for the 25% and 30% systems the storage modulus decreased dramatically above T_g thus rendering it difficult to observe any higher temperature transitions. Nevertheless there was a broad agreement between the two techniques in terms of the discontinuous (with respect to concentration) appearance of the distinct T_g events, although clearly in the present case the MTDSC response was less ambiguous and hence this data is used for subsequent quantitative analysis.

Table 1 T_g Values for Ethylcellulose Films Containing Varying Levels of FCO Obtained Using MTDSC (Derivative Reversing Heat Flow) and DMA (Tensile Mode) Methods

FCO Concentration	MTDSC (°C)	DMA (°C)
0%	129.2 ± 0.1	133.6 ± 0.3
5%	110.5 ± 0.3	121.2 ± 0.3
10%	103.8 ± 0.6	109.5 ± 0.4
15%	103.9 ± 1.2	108.4 ± 0.4
20%	54.0 ± 0.3	107.7 ± 0.7
	99.8 ± 2.1	69.8 ± 1.3
25%	53.8 ± 1.9	69.4 ± 0.3
	99.3 ± 3.9	
30%	51.0 ± 0.9	68.2 ± 0.4
	97.2 ± 1.1	

Pulsed Force Atomic Force Microscopy (AFM) and Nano-Thermal Analysis

Pulsed Force AFM

Figure 4 shows the topography and adhesion images of EC films with 10%, 20%, and 30% FCO. With 10% FCO, the films had smooth and homogenous surfaces. However, at 20% to 30% FCO levels, more features were observed on the film surface. On adding 30% FCO, evidence for phase separation was seen. More specifically, distinct regions of lower adhesion were observed which one may tentatively ascribe to the lower T_g species detected using MTDSC. It is also noted that there is evidence, albeit less clear, for such phase separation at 20% FCO. Comparison of the adhesion and topographic images indicates that there is an overlap in distribution of the phase separated regions using the two interrogation methods; this is discussed in more detail below.

Nanothermal Analysis

According to the topography and adhesion images as outlined above, films with higher level of plasticizers were observed to have a greater level of differential features on the surface. However, corresponding features were also observed on the topography images due to the height difference. This would

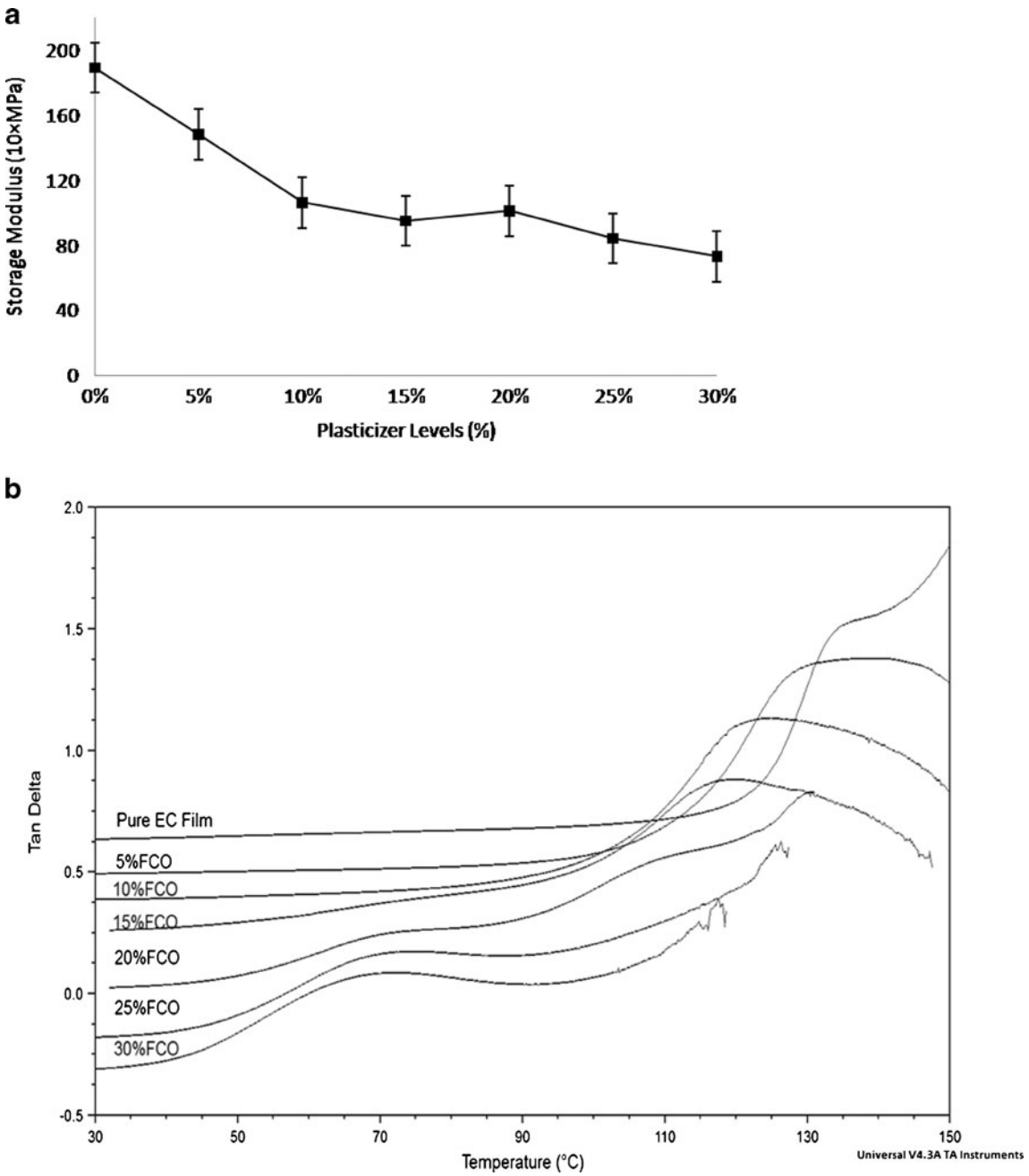

Fig. 3 (**a**) Storage modulus of ethylcellulose films containing up to 30% FCO, obtained using dynamic mechanical analysis in tensile mode at 1 Hz. (**b**) Tan delta response of ethylcellulose films containing 0, 5, 10, 15, 20, 25, 30% w/w FCO from top to bottom, obtained using dynamic mechanical analysis in tensile mode. Note the double inflection in tan δ for the 20% systems.

result in variations in sample contact with the probe, hence it is conceivable that the observed differences in adhesion were a direct result of the topographic effects and not a function of phase separation. Therefore, one could not conclude from the AFM alone that the distinct adhesion regions were solely a reflection of phase separation. It was therefore necessary to utilize a means of identifying the nature of the separated regions in a spatially resolved manner; given the nanosize nature of these regions such identification represents a significant challenge.

In order to provide structural verification of the two regions identified, nano-thermal analysis was performed in localized thermal analysis mode on 30%FCO/EC films. Topography and adhesion images were recorded using the pulse force mode AFM as before. After the scanning of AFM images, the nanoTA probe tip was located on a number of areas, as indicated in Fig. 5 using a higher magnification than used for the images in Fig. 4, which included those of supposedly high and low adhesion. The numbers and letters in the adhesion

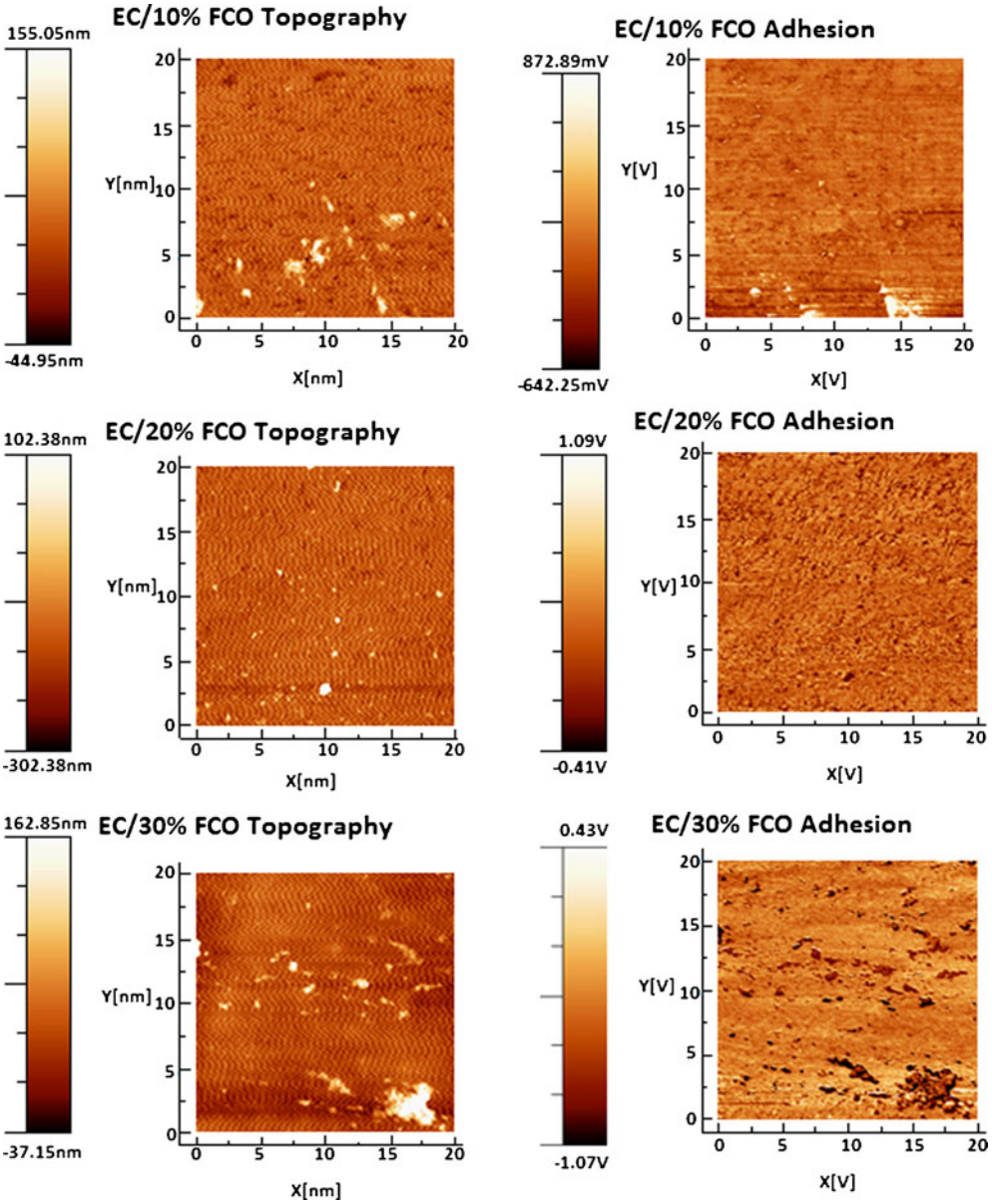

Fig. 4 Illustrative topography and adhesion (pulsed force mode, 20 μm × 20 μm) images of EC films with different concentrations of FCO at 25°C. To facilitate comparison between images, the topography scale has been set to 200 nm throughout while the adhesion scale has been set to 1.5 V.

images denote specimen locations on which local thermal analysis (LTA) studies were performed.

The corresponding LTA curves are shown in Fig. 6, in which the probe downward deflection was plotted against probe tip temperature. As the temperature increased, it is clear that sample penetration occurred as the material softened through T_g, thereby allowing a means of detecting T_g on a nanoscale via the discontinuity of probe position. The T_g was ascribed to the inflexion point of the curves. For the specific regions shown in Fig. 5, at the dark area (low adhesion) points, the T_g was circa 110°C (onset temperature) while the brighter (higher adhesion) areas had T_g values of close to 63°C.

Overall, therefore, the topography and adhesion images of the FCO/EC samples indicated that the film containing 30% FCO had areas of phase separation, although the regions being purely a function of topographic effects could not be discounted at that stage. When nanothermal analysis, and more specifically LTA, was performed on the selected areas, the T_g of the high adhesion area was similar to the low T_g observed from MTDSC and DMA while the T_g values of the lower adhesion regions were comparable to those of the high T_g obtained from MTDSC and DMA. Hence, it is now possible to correlate the two regions observed using the adhesion images to the two T_g values obtained from MTDSC.

DISCUSSION

The study has involved the combination of scanning thermal and imaging approaches to characterize the phase separation behaviour of a polymer-plasticizer system. In terms of thermal analysis, the system proved challenging in that the

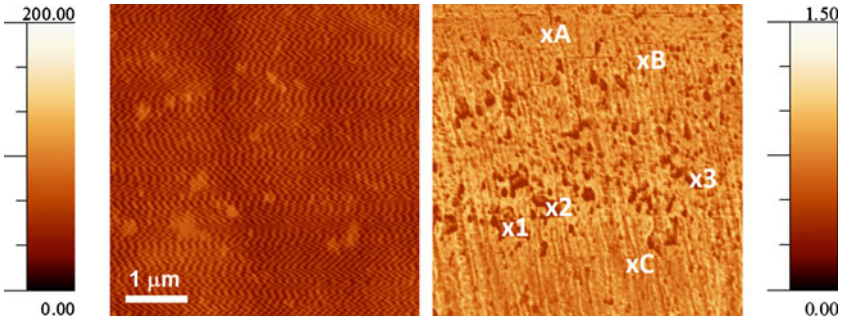

Fig. 5 Illustrative topography (left) and adhesion (right; pulsed force mode, 5 μm × 5 μm) images of EC films with 30% of FCO at 25°C. To facilitate comparison between images, the topography scale has been set to 200 nm while the adhesion scale has been set to 1.5 V. The numbers and letters (associated with the high and low T_g values, respectively, presented in Fig. 6) correspond to areas on which nanothermal analysis was subsequently performed.

heat capacity change through T_g was extremely subtle, even when using MTDSC, hence the use of the derivative signal was required. Similarly, the presence of higher temperature signals corresponding to crystallite melting (12), while probably not impinging on the present study as such, added a layer of further complexity. Indeed, the question still remains as to whether these crystallites have a significant influence on the mechanical properties of the films.

DMA studies were also not straightforward in that the films under study were, of necessity, very thin and hence did not lend themselves well to such analysis. However, the results for the T_g were broadly in agreement with those obtained from MTDSC, although our view is that the latter is a more reliable measurement approach for these systems.

The T_g measurements clearly indicated a form of phase separation, although it was similarly clear that such separation was not manifesting as simple segregation into individual components. Instead, neither of the two T_g values obtained corresponded to the pure EC. The T_g value of FCO is not known (triglycerides are reported to crystallize on cooling prior to T_g being reached); and extensive thermal studies here were not able to find a compelling T_g event. However it is highly unlikely

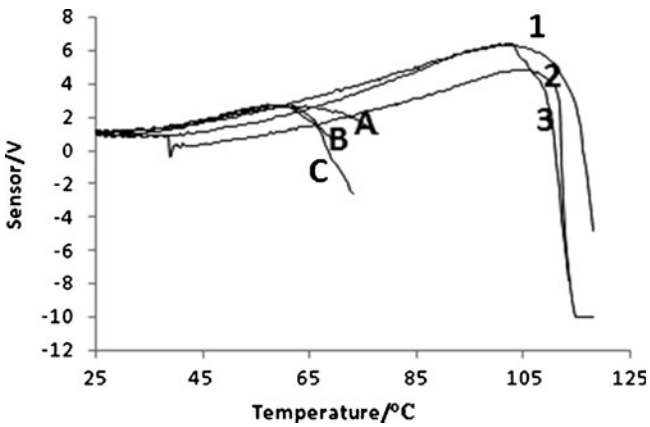

Fig. 6 Nanothermal analysis of ethylcellulose films containing 30% FCO (the numbers and letters correspond to the regions specified in Fig. 5). The sensor position is expressed as differential voltage.

that a substance that is liquid at room temperature could show a T_g at circa 50°C (and no such transition is seen for the pure material), hence we consider it very unlikely indeed that the lower transition corresponded to the glass transition of FCO.

The system separated into two conjugate phases, both of which contain both components in different proportions, one being enriched in plasticizer whilst the other is enriched in polymer. Such separation has been previously described (23), although there are other approaches to interpreting the appearance of two glass transitions. In particular, Lodge and McLeish (24) and Lodge *et al* (25) have challenged the premise of the appearance of two T_g values axiomatically indicating phase separation. They argued for a self-concentration model whereby the two components can be associated in a one phase system such that chain connectivity that allows cooperative behaviour between species even when the system may be considered to be fully miscible. In the present case, where the T_g values do not correspond to either species, these arguments are unlikely to be applicable, although the possibility of a version of such cooperative behaviour should not be excluded. Nevertheless, for the current discussion it may be assumed that the system phase separated into two conjugate systems.

Assuming the composition dependence of the T_g of EC on low additions of FCO, the Gordon Taylor equation (3) and Simha Boyer rule (26) may be used respectively

$$T_{gmix} = \frac{w_1 \cdot T_{g1} + K \cdot w_2 \cdot T_{g2}}{w_1 + K \cdot w_2} \tag{1}$$

$$K = \frac{T_{g1} \cdot \rho_1}{T_{g2} \cdot \rho_2} \tag{2}$$

where w is the weight fraction of the components, ρ is the density of the components. If Eqs. 1 and 2 are combined then the following equation can be obtained

$$T_{gmix} = \frac{w_1 \cdot T_{g1} + \frac{T_{g1} \cdot \rho_1}{\rho_2} \cdot w_2}{w_1 + \frac{T_{g1} \cdot \rho_1}{T_{g2} \cdot \rho_2} \cdot w_2} \tag{3}$$

At 5% FCO level, if we take component 1 as EC and component 2 as FCO, then T_{g1}=130°C=403.2 K; w_1= 0.95; w_2=0.05; ρ_1=1.13 mg/mL; ρ_2=0.924 mg/mL (taken from manufacturers information); $T_{gmix}=T_g$ of 5% FCO film=109.8°C=383.0 K. T_g of FCO can then be estimated using Eq. 3 as 215.2 K=-58.0°C.

By using this value we can now obtain an estimate of the compositions of the composite systems. For example, at 20% FCO levels the weight fraction of FCO in the high T_g phase can be estimated using Eq. 3 as 8%, whereas the level is 24% in the low T_g phase. The observation that the T_g values do not change indicates that the proportionality of the components within each phase stays the same, although the total quantity of each phase will vary with over composition. Again, however, one must consider the distinct possibility that the composition will alter as a function of the experimental temperature, plus the calculation of the glass transition of the FCO is very much approximate, hence one should not consider these values to be absolute in the sense of their necessarily reflecting the room temperature composition, but nevertheless the above analysis provides a basic means of making such an assessment. We suggest that high speed T_g measurements may well be a simple method whereby the T_g values could be measured in a timeframe that would not allow significant compositional change.

In terms of imaging, temperature controlled-AFM has been used on previous occasions to characterise film formation and structure. For example, Meincken and Sanderson (27) used the method to examine latex behaviour during the formation process, while Song *et al* (28) used micro-thermal analysis (the precursor technique to the nano-thermal analysis used here) to image phase separation in polymer blends, whereby the identified zones were of the order of tens of micrometers. The present study does appear to highlight some significant advantages to the nano-thermal approach, particularly when used in conjunction with MTDSC. Firstly, MTDSC clearly showed a complex phase separation/ immiscibility profile. Without this data it would be extremely difficult to interpret any accompanying imaging results, hence indicating that these two approaches are highly complementary and their simultaneous use is very advisable for these studies, despite the nano-thermal analysis being theoretically capable of producing thermal analysis data on its own. Secondly, the use of LTA studies using the nanoprobes overcomes one of the principal difficulties associated with AFM, namely the positive identification of observed structures. Previous studies (29) have indicated that the glass transitions measured using micro- and nano-thermal analysis tend to be higher than those obtained using conventional thermal techniques. This may be a result of the fast heating rates used (degrees per second rather than minute). This is necessary in order to localise heat into the region immediately adjacent to the tip, but may result in the glass transition appearing higher due to either kinetic effects or due to the process measured being softening rather than the T_g directly. However, despite these issues (and the data presented here indicates that the difference between the LTA and other thermal studies is comparatively small) it is clear that the method may identify different regions according to the associated thermal events. This is of critical importance, particularly when one considers that the method is also able to differentiate between topographic and compositional features. Indeed when used in conjunction with imaging studies the method has been shown to be able to map very subtle regional differences in terms of domain size.

Overall, therefore, this study suggests that FCO forms a conjugate, bicomponent phase system in ethylcellulose. More broadly, however, the study has demonstrated that nano-thermal analysis, in conjunction with thermal methods such as MTDSC, may provide a powerful new method of imaging regions of phase separation while also allowing identification of the observed structures.

CONCLUSIONS

The study has used a combined thermal and imaging approach to study immiscibility between a plasticizer/polymer system (fractionated coconut oil in ethylcellulose). Thermal methods revealed evidence for immiscibility, with two glass transitions noted, neither of which corresponded to the T_g of either pure component. It was suggested that this indicated a conjugate system, whereby the phase separation manifests as two phases containing both components. Nanothermal analysis allowed both mapping and localized thermal analysis to be performed, the latter verifying the structural nature of the regions noted using pulsed force imaging in that thermal events were noted associated with low and high adhesion regions which corresponded well to the two transitions observed using MTDSC. It is suggested that this method allows not only imaging and identification of distinct structures but also positive identification of the nature of those structures.

ACKNOWLEDGEMENT

We would like to thank Colorcon Ltd. for financial support.

REFERENCES

1. Repka MA, Majumdar S, Battu SK, *et al.* Applications of hot-melt extrusion for drug delivery. Exp Opinion Drug Del. 2008;5 (12):1357–76.

2. Rajabi-Siahboomi AR, Farrell TP. The applications of formulated systems for the aqueous film coating of pharmaceutical oral solid dosage forms. In: Felton L, McGinity J, editors. Aqueous polymeric coatings for pharmaceutical dosage forms. 3rd ed. New York: Informa Healthcare; 2008. pp. 323–344.
3. Gordon M, Taylor JS. Ideal polymers and the second-order transitions of synthetic rubbers: non-crystalline copolymers. Journal of Application Chemistry. 1952;2:493–500.
4. Marcilla A, Beltran M. Mechanisms of plasticizers action. In: Wypych G, editor. Handbook of plasticizers. Toronto: ChemTec Publishing; 2004. p. 107–21.
5. Sears JK, Darby JR. Technology of plasticizers. New York: John Wiley and Sons; 1982.
6. Fox TG, Flory PJ. Second-order transition temperatures and related properties of polystyrene. J Appl Phys. 1950;21:581–91.
7. Flory PJ. Principles of polymer chemistry. Thaca, New York: Cornell University Press; 1953.
8. DiPaola-Baranyi G, Guillet JE. Estimation of polymer solubility parameters by gas-chromatography. Macromolecules. 1978;11:228–35.
9. Qi S, Belton P, Nollenberger K, Clayden N, Reading M, Craig DQM. Characterisation and prediction of phase separation in hot-melt extruded solid dispersions: a thermal, microscopic and NMR relaxometry study. Pharm Res. 2010;27(9):1869–83.
10. Widjaja E, Kanaujia P, Lau G, Ng WK, Garland M, Saal C, Hanefeld A, Fischbach M, Maio M, Tan RBH. Detection of trace crystallinity in an amorphous system using raman microscopy and chemometric analysis. Eur J Pharm Sci. 2011;42(1–2):45–54.
11. Qi S, Gryczke A, Belton P, Craig DQM. Characterisation of solid dispersions of paracetamol and eudragit (R) E prepared by hot-melt extrusion using thermal, microthermal and spectroscopic analysis. Int J Pharm. 2008;354(1–2):158–67.
12. Lai H-L, Pitt Kl, Craig DQM. Characterisation of the thermal properties of ethylcellulose using differential scanning and quasi-isothermal calorimetric approaches. Int J Pharm. 2010;386:178–84.
13. Bheda J, Fellers JF, White JL. Phase-behaviour and structure of liquid crystalline solutions of cellulose dderivatives colloid. Polym Sci. 1980;258:1335–42.
14. Harding L, King WP, Dai X, Craig DQM, Reading M. Nanoscale characterisation and imaging of partially amorphous materials using local thermomechanical analysis and heated tip AFM. Pharm Res. 2007;24(11):2048–54.
15. Nelson BA, King WP. Measuring material softening with nanoscale spatial resolution using heated silicon probes. Rev Sci Instrum. 2007;78(2):023702.
16. Harding L, Wood J, Reading M, Craig DQM. Two- and three-dimensional imaging of multicomponent systems using scanning thermal microscopy and localized thermomechanical analysis. Anal Chem. 2007;79(1):129–39.
17. Hammiche A, Bozec L, Pollock HM, German M, Reading M. Progress in near-field photothermal infra-red microspectroscopy. J Microsc Oxford. 2004;213:129–34.
18. Mrklic Z, Rusic D, Kovacic T. Kinetic model of the evaporation process of benzylbutyl phthalate from plasticized poly(vinyl chloride). Thermochim Acta. 2004;414(2):167–75.
19. Reading M, Luget A, Wilson R. Modulated differential scanning calorimetry. Thermochim Acta. 1994;238:295–307.
20. Baiardo M, Frisoni G, Scandola M, Rimelen M, Lips D, Ruffieux K, Wintermantel E. Thermal and mechanical properties of plasticized poly(L-lactic acid). J Appl Polym Sci. 2003;90:1731–8.
21. Okamoto K, Ichikawa T, Yokohara T, Yamaguchi M. Miscibility, mechanical and thermal properties of poly(lactic acid)/polyester-diol blends. Eur Polym J. 2009;45:2304–12.
22. Jia Z, Tan J, Han C, Yang Y, Dong L. Poly(ethylene glycol-*co*-propylene glycol) as a macromolecular plasticizing agent for polylactide: thermomechanical properties and aging. J Appl Polym Sci. 2009;114:1105–17.
23. Senichev VY, Tereshatov VV. Theories of compatibility. In: Wypych G, editor. Handbook of plasticizers. Toronto: ChemTec Publishing; 2004. p. 121–50.
24. Lodge TP, McLeish TCB. Self-concentrations and effective glass transition temperatures in polymer blends. Macromolecules. 2000;33:5278–84.
25. Lodge TP, Wood ER, Haley JC. Two calorimetric glass transitions do not necessarily indicate immiscibility: the case of PEO/PMMA. J Polym Sci, Part B: Poly Phys. 2006;44:756–63.
26. Simha R, Boyer RF. On a general relation involving the glass temperature and efficients of expansion of polymers. J Chem Phys. 1962;37:1003–7.
27. Meincken M, Sanderson RD. Determination of the influence of the polymer structure and particle size on the film formation process of polymers by atomic force microscopy. Polymer. 2002;43(18):4947–55.
28. Song M, Hourston DJ, Grandy DB, Reading M. An application of micro-thermal analysis to polymer blends. J Appl Polym Sci. 2001;81:2136–41.
29. Royall PG, Kett VL, Andrews CS, Craig DQM. Identification of crystalline and amorphous regions in low molecular weight materials using microthermal analysis. J Phys Chem B. 2001;105:7021–6.